METROLOGY AND MEASUREMENT SYSTEMS
Index 330930, ISSN 0860-8229
www.metrology.pg.gda.pl

A NOVEL METHOD FOR 3D MEASUREMENT OF RFID MULTI-TAG NETWORK USING A MACHINE VISION SYSTEM

Xiao Zhuang[1,2)], Xiaolei Yu[1,2)], Zhimin Zhao[1)], Wenjie Zhang[1)], Zhenlu Liu[1)], Dongsheng Lu[1)], Dingbang Dong[1)]

1) *Nanjing University of Aeronautics and Astronautics, College of Science, Nanjing 210016, People's Republic of China* (✉ *nuaaxiaoleiyu@126.com*, 86 177 0518 0262, *nuaaxiaoleiyu@126.com*, *nuaazhzhm@126.com*, *jiewenz@163.com*, *550138109@qq.com*, *1174889695@qq.com*, *1747758873@qq.com*)
2) *National Quality Supervision and Testing Center for RFID Product, Jiangsu, Nanjing 210029, People's Republic of China*

Abstract

The three-dimensional (3D) coordinate measurement of *radio frequency identification* (RFID) multi-tag networks is one of the important issues in the field of RFID, which affects the reading performance of RFID multi-tag networks. In this paper, a novel method for 3D coordinate measurement of RFID multi-tag networks is proposed. A dual-CCD system (vertical and horizontal cameras) is used to obtain images of RFID multi-tag networks from different angles. The iterative threshold segmentation and the morphological filtering method are used to process the images. The template matching method is respectively used to determine the *two-dimensional* (2D) coordinate and the vertical coordinate of each tag. After that, the 3D coordinate of each tag is obtained. Finally, a *back-propagation* (BP) neural network is used to model the nonlinear relationship between the RFID multi-tag network and the corresponding reading distance. The BP neural network can predict the reading distances of unknown tag groups and find out the optimal distribution structure of the tag groups corresponding to the maximum reading distance. In the future work, the corresponding in-depth research on the neural network to adjust the distribution of tags will be done.

Keywords: 3D measurement, RFID multi-tag network, dual-CCD system, neural network, machine vision.

1. Introduction

In the field of radio *frequency identification* (RFID), the three-dimensional (3D) distribution of RFID multi-tag networks has a significant impact on its reading performance. So, in order to improve the reading performance of an RFID system in the practical engineering application, the 3D coordinates of the RFID multi-tag networks must be measured. In the recent years, a camera for the object measurement has been widely applied [1, 2]. In [3], Mi-Seon Kang proposed a new calibration method for inspecting 3D objects using a single camera. A machine-vision-based approach to radial error measurement of a lathe spindle using a CMOS camera and a PC-based image processing system was presented in [4]. In [5], a novel approach to measuring the object size using a regular digital camera was proposed. The proposed method was based on a new depth-information extraction scheme using a regular digital camera. Feng presented a novel

Article history: received on Oct. 30, 2017; accepted on Mar. 24, 2018; available online on Sep. 30, 2018, DOI: 10.24425/123898.

high-speed real-time technique for measuring 3D coordinates, based on fringe projection with consideration of the camera lens distortion [6]. Chen proposed a novel non-contact, full-field, 3D, multi-camera *digital image correlation* (DIC) measurement system [7]. Su presented an economic real-time system for tracking a fast moving object using adjacent inexpensive multiple web cameras [8]. Comparing with the use of a single camera for the 3D coordinate measurement, the time consumed using two cameras to achieve the target 3D coordinate measurement is less and the operation is simple. Besides that, comparing with using three and multiple cameras, using two cameras has been able to meet the 3D coordinate measurement requirements, and the measurement cost is low. So, two CCD cameras (vertical and horizontal ones) are used to measure the 3D coordinates of RFID tags.

RFID technology is a wireless communication technology, which has been widely used in many fields [9]. An important advantage of RFID technology is the simultaneous recognition of multiple targets. However, in order to achieve simultaneous recognition of multiple targets, it is necessary to face the problem of how to improve the performance of tag reading. Nowadays, the commonly used approach to improve the tag reading ability is to use an anti-collision algorithm to solve the data conflicts caused by multiple tags existing in the same *radio frequency* (RF) channel at the same time, such as ALOHA algorithm and the binary tree algorithm [10–12]. Although these algorithms solve the collision problem in the communication protocol layer, they could not deal with the impact of actual external interference on the air communication.

Some scholars have researched the optimization of RFID tag distribution. In the reference [13], Ni L.M. presented LANDMARC: a location sensing prototype system that uses RFID technology for locating objects inside buildings. The major advantage of LANDMARC is that it improves the overall accuracy of locating objects by utilizing the concept of reference tags. However, because of irregularity of the tags' arrangement, the locating performance of LANDMARC has been affected. Zhao Y. proposed the VIRE approach to locate objects inside buildings in which the tags were set as a regular polygon [14]. A 2D localization system based on the phase-of-arrival evaluation of passive *ultrahigh frequency* (UHF) RFID transponders was presented and several tags were arranged to create a uniform linear array in order to handle the ambiguity caused by the phase evaluation [15]. Nevertheless, the tag signals interfered with each other due to the corresponding distribution. In [16], Yu calculated the extremum of azimuth matrix and obtained the optimal geometric distribution of tags in the Fisher matrix of evaluation. The work optimized the tags' distribution to improve the reading performance of RFID system in theory. However, the research reported in [16] was only analysed in theory, not in a practical application. Based on the above research, the paper applies an image processing method to improve the acquisition efficiency of the 3D coordinates of RFID tags, which could provide the data support for the subsequent BP neural network analysis to optimize the tag distribution and improve the reading performance of RFID system in a practical application. Firstly, the horizontal and vertical cameras are used to obtain the images of RFID tags from different angles. Then, on the basis of image processing, the 3D coordinates of the tags are determined with a template matching method. Finally, a BP neural network is used to model the nonlinear relationship between the RFID multi-tag network and the corresponding reading distance. The BP neural network can predict the reading distances of unknown tag groups and find out the optimal distribution structure of the tag groups corresponding to the maximum reading distance. Compared with the corresponding system, the proposed system has three advantages. Firstly, the proposed system can prevent the electromagnetic interference in a dynamic environment, which could easily affect the direct measurement results obtained by antennas. Secondly, the image processing results can be combined with the subsequent BP neural network analysis to obtain the relationship between the node network of multi-tags and the reading performance of RFID system. Thirdly, the use

of two cameras improves the acquisition efficiency of the 3D coordinates of RFID tags, which provides the data support for the subsequent optimization of tag distribution. However, as the proposed system is still in the laboratory research stage, the system contains multiple modules and algorithms. Therefore, the system is complicated in the process of RFID tag 3D measurement. The real-time performance needs to be improved. The research on the real-time and system integration will follow in the future.

2. Design of measurement system

2.1. Design of illumination system

In order to better select a light source, we compare the main characteristics of several common light sources in Table 1. In view of the content of Table 1, we find that the LED light source performs better, featuring high design freedom, high wavelength selection, fast response, long service life and so on. So, the illumination system is designed using LED as the light source.

Table 1. Comparison of several common light sources.

Serial no	Compare items	Energy-saving fluorescent light	High pressure sodium light	Metal halide light	LED light	Electrodeless light
1	lifetime/h	About 12000 h	About 20000 h	About 10000 h	About 50000 h	About 60000 h
2	The whole light effect /(lm/w)	90~100	100~120	85~100	100~110	90~100
3	Light failure /%	5%	10%	25%	3%	5%
4	Color rendering	> 80	20~25	60~65	>80	>80
5	Start the stabilization time	1~3 s	4~8 min	10~15 min	Instantaneous	Instantaneous
6	Restart time /min	Instantaneous	10~15	10~15	Instantaneous	Instantaneous
7	Color temperature (k)	3000~6000 (Optional)	About 2000	3000~4000 (Optional)	3500~7000 (Optional)	2700~6500 (Optional)
8	Strobe	yes	yes	yes	no	no

The illumination system uses a broad spectrum of white light LEDs as a luminous material. The light source is a combination of two-LED array strip. When the LED array is installed on the mechanical platform of an electro-optical system, the LED array on each side is independently illuminated. The details of illumination system are as follows: type: T5E10, power: 12 W, beam angle: 120°, luminous flux: 1080 lm, colour temperature: 6000 K. The angle and power can be adjusted according to the target. The illumination system is shown in Fig. 1 and Fig. 2.

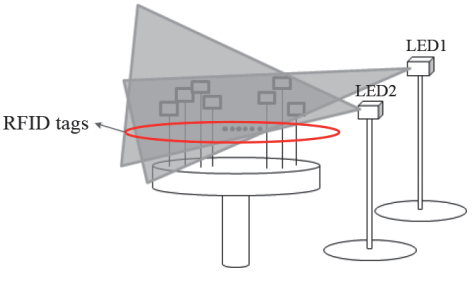

Fig. 1. The whole frame of the illumination system.

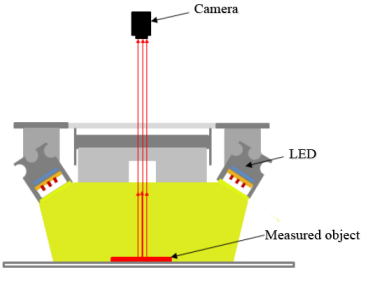

Fig. 2. The illumination system design.

2.2. Design of measurement system

2.2.1. Construction of measurement platform

A schematic diagram of the dual-CCD semi-physical measurement platform is shown in Fig. 3, and its photo – in Fig. 4. The measurement platform consists of a reader, a reader antenna, an RFID tag, an RFID tag bracket, a control computer, a servomotor, a vertical camera, a horizontal camera, an illumination system, a guide rail and a turntable. The bottom of the RFID tag bracket is labelled. The RFID reader is connected to the reader antenna and the control computer. The vertical and horizontal cameras are connected to the control computer.

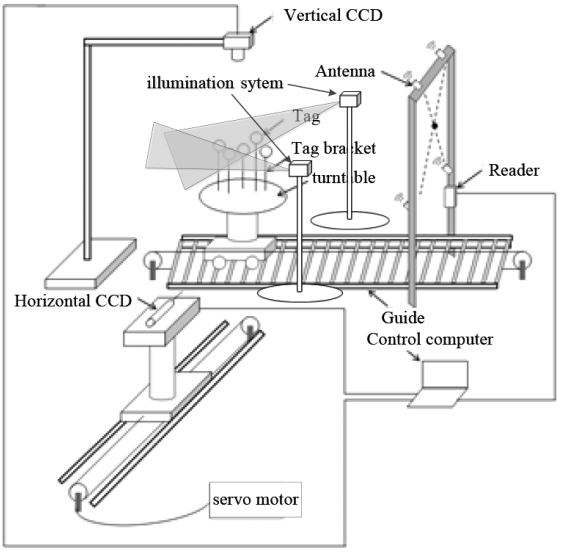

Fig. 3. A schematic diagram of the dual-CCD semi-physical measurement platform.

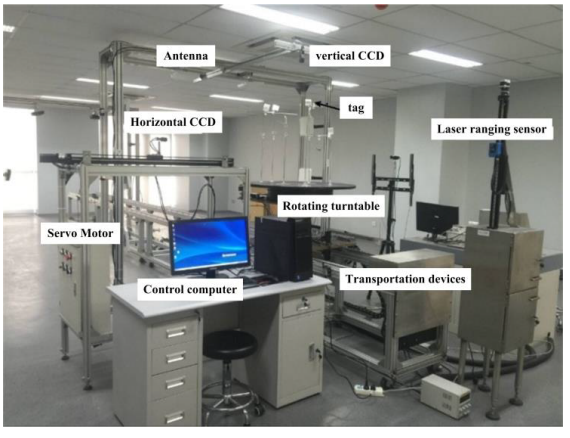

Fig. 4. A photo of the semi-physical platform for 3D measurement of RFID tags.

The semi-physical test platform consists of an image acquisition system and a tag reading distance dynamic testing system. The theoretical range of operational distance is 0~10 m.

However, after performing the measurement experiments indoors, the range of operating distance has been limited to 0~4 m. An RFID tag uses UHF RFID tags – H47. The size of CCD camera is 1288×964 pixels. The size of pixel is 3.75×3.75 μm. The CCD's frame rate is 30 FPS. The readers use an Impinj Speedway Revolution R420 reader. The reader antenna uses a Laird A9028 far field antenna. The maximum RF output power of the reader antenna is 30 dBm.

2.2.2. Measurement process

The whole test platform is used for 3D coordinate measurement of RFID tags. The test flow is shown in Fig. 5. A number of brackets with RFID tags are placed on the turntable. The dynamic tag reading distance testing system is started to obtain the reading distance of tag distribution. The control computer controls the vertical and horizontal cameras to collect images of the turntable and tags. The obtained images are stored in the control computer. Then, the template matching method is used to obtain the 2D coordinate and vertical coordinate of each tag. Eventually, the 3D coordinate of each tag is obtained.

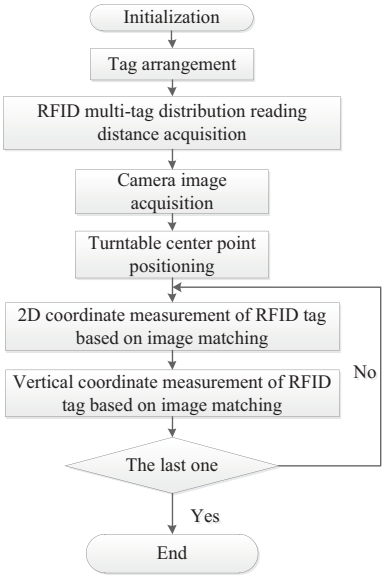

Fig. 5. A flowchart of RFID tag 3D measurement.

3. 3D coordinate measurement of RFID tags

3.1. Image matching

In order to measure 3D coordinates of RFID tags, an image matching method is needed. The template matching method is used to match the tag images with the template. Firstly, we select an image ($M \times N$ pixels) as the matching template. Secondly, in the target image, a matching point is determined, which is called the target point. With the target point as the centre, $M \times N$ pixel grey-scale arrays can be obtained from the $K \times L$ ($K > M$, $L > N$) pixel search area of the target image. All $M \times N$ pixel grey-scale arrays are sequentially taken out from the search area. The correlation coefficients of the grey-scale arrays and the template are calculated one by one.

When the correlation coefficient reaches a certain threshold (0.7), the search window area is determined as the matching region. When the correlation coefficient of the grey-scale array and the temple is bigger than 0.7, the matching is successful. Otherwise, the matching fails. A diagram of the template matching principle is shown in Fig. 6. Through the template matching, a matching region can be found in the image.

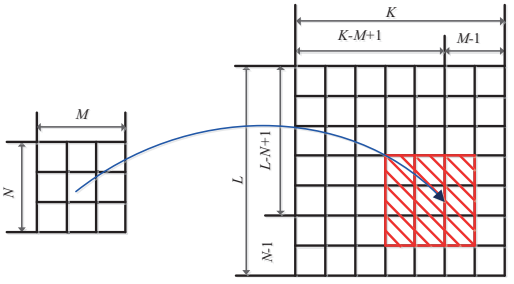

Fig. 6. A diagram of the template matching principle.

3.2. 2D coordinate measurement of RFID tag

In order to obtain 2D coordinates of RFID tags, the iterative threshold segmentation and the morphological filtering method are used to process the image. The iterative threshold segmentation is used to obtain the binary image of the turntable. The morphological filtering method is used to corrode and inflate the binary image to obtain the fill image of the turntable. The structural element used for corrosion and expansion is a disk with a radius of 11. The origin of the turntable is calculated, which is shown in Fig. 7 a–d. Then, a polar coordinate system is established with the direction of the horizontal camera as the polar axis in Fig. 7d.

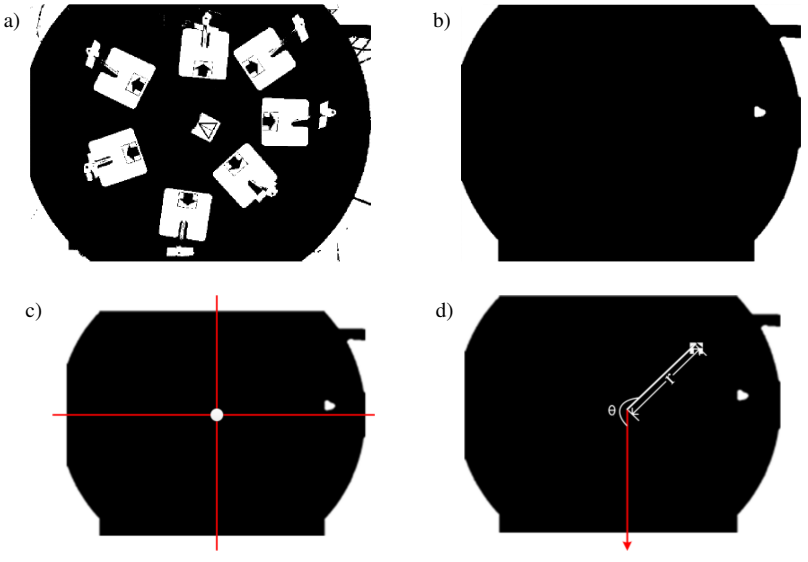

Fig. 7. The centre point location of the turntable and establishment of a polar coordinate system. A binary image of the iterative threshold segmentation (a); the result of the morphological filtering method (b); The centre point location of the turntable (c); schematic diagram of the polar coordinate system (d).

The RFID tags are placed on the turntable. The mark point is pasted at the bottom of each tag. One of the mark points is selected as the mark point template. Each tag's mark point is matched with the template. The matching results are shown in Fig. 8. Through the template matching, each tag's position is recognized. The distance between each tag's mark point and the centre of the turntable is denoted as r. The i_{th} tag's distance is recorded as r_i.

Fig. 8. Matching results of bottom mark points of 7 tags.

3.2.1. Horizontal camera controlling

Firstly, we use the control computer to adjust the horizontal camera so that it is positioned at the centre of the guide rail. It is adjusted so that it can clearly focus on the i_{th} tag. It collects the image of the i_{th} tag. The distance d_i between the i_{th} tag and the horizontal camera is calculated with (1):

$$d_i = L_1 - r_i\,, \tag{1}$$

where L_1 is the distance from the horizontal camera to the centre of the turntable. r_i is the distance from the i_{th} tag's mark point to the centre of the turntable.

Afterwards, we calculate the object distance l_i, which is required by the horizontal camera for the i_{th} RFID tag:

$$l_i = \frac{fl'}{l' - f}\,, \tag{2}$$

where l' is the distance between the lens and the CCD sensor inside the horizontal camera, f is the focal length of the horizontal camera.

Finally, the distance ΔL_i needed to be adjusted for the horizontal camera is calculated with (3):

$$\Delta L_i = d_i - l_i\,. \tag{3}$$

If ΔL_i is larger than zero, the horizontal camera approaches the tag. Otherwise, the horizontal camera moves away from the tag.

3.2.2. 2D coordinate measurement of RFID tag

The control computer adjusts the servomotor to drive the turntable to rotate. The horizontal camera is adjusted so that it can clearly focus on the i_{th} tag. The angle at which the i_{th} tag turns is the polar angle θ_i. The θ_i and the above r_i are the i_{th} RFID tag's 2D coordinate parameters. The 2D coordinate of the i_{th} RFID tag is further calculated as $(r_i \cos\theta_i, r_i \sin\theta_i)$. The above steps in Subsection 3.2 should be repeated to calculate each tag's horizontal 2D coordinate.

3.3. Vertical coordinate measurement of RFID tag

After obtaining the 2D coordinates of RFID tags, one of the tags is selected as the template. The distance from the centre of the template to the turntable is calculated as the vertical coordinate of the template. The control computer controls the servomotor to drive the turntable to rotate. The horizontal camera is adjusted so that it can clearly focus on the template. The image of the template is collected in the control computer. The image cropping method is used to process the template image. The horizontal camera is adjusted to obtain clearly each tag's image. The obtained images are sequentially taken out to match with the template image. The matching results of the first tag group are shown in Fig. 9.

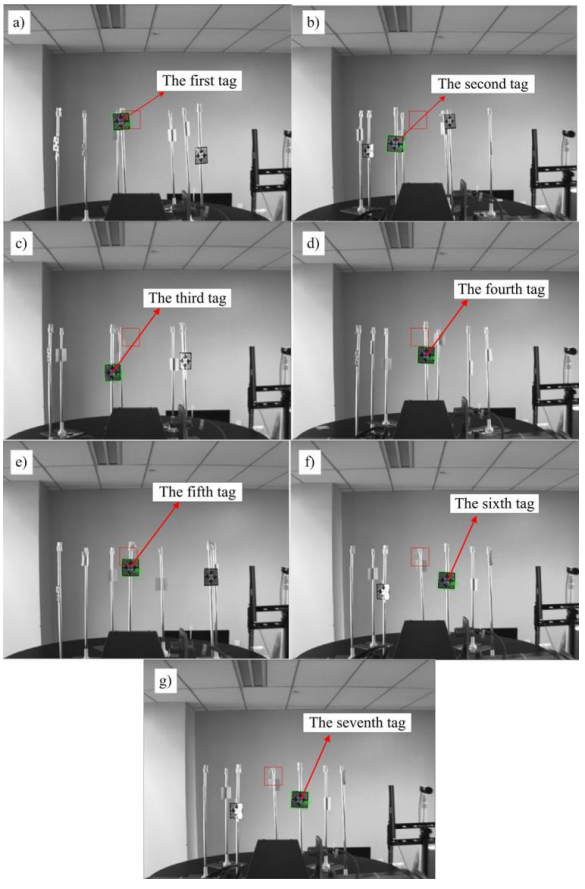

Fig. 9. The results of matching seven tags in the vertical direction. Tag 1 (a); Tag 2 (b); Tag 3 (c); Tag 4 (d); Tag 5 (e); Tag 6 (f); Tag 7 (g).

After successful matching, the numbers of pixels between the centres of measured tags and the template are calculated. Because the size of each pixel in the CCD is known and the distance between the image plane and the horizontal camera is fixed, the size of each pixel in the image can be determined by the triangle similarity relation. According to the difference in the number of pixels in the vertical direction between a measured tag and the template, the relative

distance between the measured tag and the template in the vertical direction can be determined. A schematic diagram of the similarity relation is shown in Fig. 10:

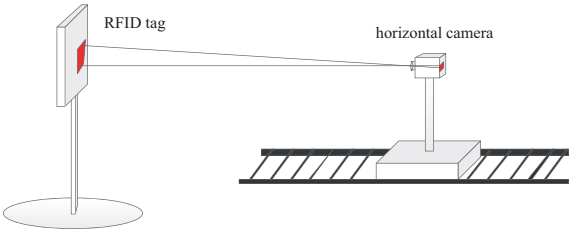

Fig. 10. A sketch map of the similarity relation.

The relation of coordinates is given by the following equation:

$$H_i = h \pm c_i \times a, \tag{4}$$

where H_i is the vertical coordinate of the i_{th} tag. h is the vertical coordinate of the template. a is the length of the image pixel. c_i is the number of pixels between the centre point of the i_{th} RFID tag and the centre point of the template. When the centre point of thei_{th} RFID tag is below the centre of the template, the (4) takes the "$-$" sign. When the centre point of thei_{th} RFID tag is above the centre of the template, the (4) takes the "$+$" sign.

4. RFID multi-tag neural network

In order to obtain the optimal tag distribution network corresponding to the maximum reading distance, the mass distribution network and the corresponding reading distances must be tested. In order to quickly identify and optimize the network distribution structure of the tags in a practical application, it is necessary to establish a nonlinear relation model between the tag network distribution structure and the reading distance, *i.e.* a nonlinear relation model between the 3D coordinates of the tag groups and the corresponding reading distances. Considering the time consumption of different methods presented in Table 2, the paper just uses a simple BP neural network to model the nonlinear relationship between the 3D coordinates of the tag groups and the corresponding reading distances. The time consumed by the BP neural network analysis in this paper is only 10.31 s. The neural network is trained with 100 sets of data, and the trained network is used to predict the reading distances of 28 tag groups. The prediction error of BP neural network is defined as (5):

$$E = \frac{d_p - d_r}{d_r} \times 100\%. \tag{5}$$

The values of BP neural network prediction error are shown in Table 2 and Fig. 11.

Table 2. Time consumed by different methods for the training data in this paper.

Methods	Average time consuming (s)
BP neural network	10.31
GA-BP neural network	216.59
PSO-BP neural network	229.67

It can be seen from the above results that the BP neural network can basically predict the reading distances of the tag groups. The maximum reading distance is 1.8751, and its corresponding optimal tag network distribution structure is shown in Fig. 12.

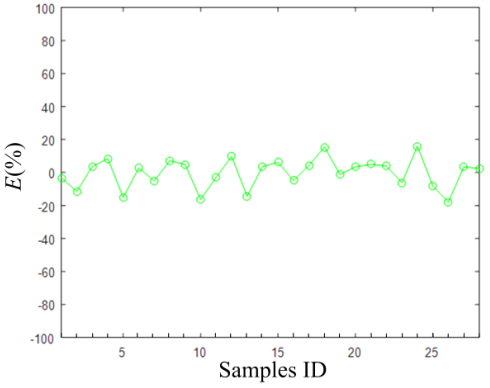

Fig. 11. Error values of BP neural network prediction.

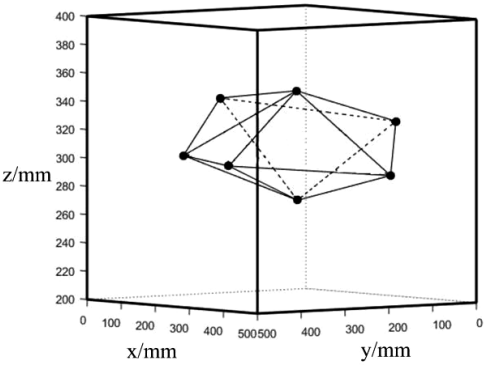

Fig. 12. The optimal structure of RFID tag network.

It can be seen from Table 3, Fig. 11 and Fig. 12 that the BP neural network can effectively predict the reading distances of tag groups and find out the optimal distribution structure of tag groups corresponding to the maximum reading distance.

Table 3. BP neural network prediction results of the reading distances in RFID systems.

Sample ID	x_1/m	y_1/m	z_1/m	...	x_7/m	y_7/m	z_7/m	d_r/m	d_p/m	E (%)
1	0.2101	−0.0188	0.3019	...	0.2192	−0.2254	0.3801	2.00	1.8751	−3.35
2	0.1248	0.0367	0.3075	...	0.1072	−0.1944	0.3032	1.94	1.1688	−11.45
3	0.1653	0.1319	0.2555	...	0.0682	−0.1079	0.3070	1.32	1.1406	3.69
	⋮	⋮	⋮	...	⋮	⋮	⋮	⋮	⋮	⋮
26	0.1682	0.0137	0.3161	...	0.0644	−0.1748	0.3102	1.11	1.0913	−17.95
27	0.0374	0.1467	0.3495	...	0.1674	−0.0121	0.3158	1.36	1.3553	3.46
28	0.1454	0.0359	0.3497	...	0.0712	−0.1514	0.3147	1.68	1.8014	24.24

5. Conclusion

In this paper, a 3D coordinate measurement system of RFID multi-tag network based on a dual-CCD system is designed, and the 3D coordinates of RFID multi-tag networks are measured by the image method. After that, a BP neural network is used to model the nonlinear relationship between the 3D coordinates of RFID tags and corresponding reading distances. The BP neural network can predict the reading distances of unknown tag groups and find out the optimal distribution structure of the tag groups corresponding to the maximum reading distance. The proposed system can prevent the electromagnetic interference in a dynamic environment and improve the acquisition efficiency of the 3D coordinates of RFID tags, which provides the data support for the subsequent analysis. The proposed method can be used to optimize the distribution of RFID multi-tag networks in a practical engineering application, which could improve

the reading performance of RFID multi-tag networks. The research results are valuable for engineering applications. However, as the proposed system is still in the laboratory research stage, the further study is needed to improve the real-time performance of the system. Meanwhile, the corresponding in-depth research on the neural network to adjust the distribution of tags is required.

Acknowledgements

The work has been financially supported by the National Natural Science Foundation of China under Grant No. 61771240; China Postdoctoral Science Foundation under Grant No. 2015M580422 & No. 2016T90452; Jiangsu Province Natural Science Foundation for Youths under Grant No. BK20141032; Science and Technology Project of AQSIQ under Grant 2017QK117 & 2013QK194, as well as the 352 Talent Project of Jiangsu Bureau of Quality and Technical Supervision.

References

[1] Su, X., Zhang, Q. (2010). Dynamic 3-D shape measurement method: a review. *Optics and Lasers in Engineering*, 48(2), 191–204.

[2] Gibson, R., Atkinson, R., Gordon, J. (2016). A review of underwater stereo-image measurement for marine biology and ecology applications. *Oceanography and marine biology: an annual review*, 47, 257–292.

[3] Kang, M.S., Lee, C.H., You, B.M., Chung, Y.S. (2015). A 3D object measurement method using a single view camera. *IEEE, Information and Communication Technology Convergence*, Jeju, South Korea, 790–792.

[4] Kavitha, C., Ashok, S.D. (2017). A new approach to spindle radial error evaluation using a machine vision system. *Metrol. Meas. Syst.*, 24(1), 201–219.

[5] Pu, L., Tian, R., Wu, H.C., Yan, K. (2016). Novel object-size measurement using the digital camera. *IEEE, Advanced Information Management, Communicates, Electronic and Automation Control Conference*. Xi'an, China, 543–548.

[6] Feng, S., Chen, Q., Zuo, C., Sun, J., Yu, S.L. (2014). High-speed real-time 3-D coordinates measurement based on fringe projection profilometry considering camera lens distortion. *Optics Communications*, 329, 44–56.

[7] Chen, F., Chen, X., Xie, X., Feng, X., Yang, L. (2013). Full-field 3D measurement using multi-camera digital image correlation system. *Optics and Lasers in Engineering*, 51(9), 1044–1052.

[8] You, S.J., Truong, P.H., Ji, S.H., Lee, S.M., Lee, C.E., Cho, Y.J. (2014). A cooperative multi-camera system for tracking a fast moving object. *IEEE, Cyber Technology in Automation, Control, and Intelligent Systems*. Hong Kong, China, 141–145.

[9] Valero, E., Adán, A., Cerrada, C. (2015). Evolution of RFID applications in construction: a literature review. *Sensors*, 15(7), 15988-16008.

[10] Li, Z., He, C., Li, J., Huang, X. (2014). RFID reader anti-collision algorithm using adaptive hierarchical artificial immune system. *Expert Systems with Applications*, 41(5), 2126–2133.

[11] Joo, Y.I., Seo, D.H., Kim, J.W. (2014). An efficient anti-collision protocol for fast identification of RFID tags. *Wireless personal communications*, 77(1), 767–775.

[12] Myung, J., Lee, W., Srivastava, J. (2006). Adaptive binary splitting for efficient RFID tag anti-collision. *IEEE communications letters*, 10(3), 144–146.

[13] Ni, L.M., Liu, Y., Lau, Y.C., Patil, A.P. (2004). LANDMARC: Indoor location sensing using active RFID. *Wireless networks*, 10(6), 701–710.

[14] Zhao, Y., Ni, L.M. (2013). VIRE: Virtual reference elimination for active RFID-based localization. *Adhoc & Sensor Wireless Networks*, 17, 169–191.

[15] Scherhäufl, M., Pichler, M., Stelzer, A. (2015). UHF RFID localization based on phase evaluation of passive tag arrays. *IEEE Transactions on Instrumentation and Measurement*, 64(4), 913–922.

[16] Yu, Y., Yu, X., Zhao, Z., Liu, J., Wang, D. (2016). Measurement uncertainty limit analysis of biased estimators in RFID multiple tags system. *IET Science, Measurement & Technology*, 10(5), 449–455.